Characterization of the Desulfovibrio desulfuricans ATCC 27774 DsrMKJOP ComplexA Membrane-Bound Redox Complex Involved in the Sulfate Respiratory Pathway

ARTICLE *in* BIOCHEMISTRY · FEBRUARY 2006

Impact Factor: 3.02 · DOI: 10.1021/bi0515265 · Source: PubMed

6 AUTHORS, INCLUDING:

Ricardo H. Pires
University of Greifswald
14 PUBLICATIONS **167** CITATIONS
SEE PROFILE

Sofia Venceslau
New University of Lisbon
22 PUBLICATIONS **424** CITATIONS
SEE PROFILE

Miguel Teixeira
New University of Lisbon
282 PUBLICATIONS **7,427** CITATIONS
SEE PROFILE

Inês Cardoso Pereira
New University of Lisbon
99 PUBLICATIONS **2,155** CITATIONS
SEE PROFILE

Characterization of the *Desulfovibrio desulfuricans* ATCC 27774 DsrMKJOP Complex—A Membrane-Bound Redox Complex Involved in the Sulfate Respiratory Pathway

Ricardo H. Pires, Sofia S. Venceslau, Francisco Morais, Miguel Teixeira, António V. Xavier, and Inês A. C. Pereira*

Instituto de Tecnologia Química e Biológica, Universidade Nova de Lisboa, 2781-901 Oeiras, Portugal

Received August 1, 2005; Revised Manuscript Received September 22, 2005

ABSTRACT: Sulfate-reducing organisms use sulfate as an electron acceptor in an anaerobic respiratory process. Despite their ubiquitous occurrence, sulfate respiration is still poorly characterized. Genome analysis of sulfate-reducing organisms sequenced to date permitted the identification of only two strictly conserved membrane complexes. We report here the purification and characterization of one of these complexes, DsrMKJOP, from *Desulfovibrio desulfuricans* ATCC 27774. The complex has hemes of the *c* and *b* types and several iron−sulfur centers. The corresponding genes in the genome of *Desulfovibrio vulgaris* were analyzed. *dsrM* encodes an integral membrane cytochrome *b*; *dsrK* encodes a protein homologous to the HdrD subunit of heterodisulfide reductase; *dsrJ* encodes a triheme periplasmic cytochrome *c*; *dsrO* encodes a periplasmic FeS protein; and *dsrM* encodes another integral membrane protein. Sequence analysis and EPR studies indicate that DsrJ belongs to a novel family of multiheme cytochromes *c* and that its three hemes have different types of coordination, one bis-His, one His/Met, and the third a very unusual His/Cys coordination. The His/Cys-coordinated heme is only partially reduced by dithionite. About 40% of the hemes are reduced by menadiol, but no reduction is observed upon treatment with H_2 and hydrogenase, irrespective of the presence of cytochrome c_3. The aerobically isolated Dsr complex displays an EPR signal with similar characteristics to the catalytic $[4Fe-4S]^{3+}$ species observed in heterodisulfide reductases. Further five different $[4Fe-4S]^{2+/1+}$ centers are observed during a redox titration followed by EPR. The role of the DsrMKJOP complex in the sulfate respiratory chain of *Desulfovibrio* spp. is discussed.

Sulfate is one of the most common electron acceptors for anaerobic respiration. Sulfate-reducing organisms (*1*) are ubiquitous in a variety of anaerobic environments such as soil, sediments, marine and freshwaters, and the mouth and gut of many animals, including humans. They make a very important contribution to the global cycling of carbon and sulfur in these anaerobic environments and particularly so in marine habitats, because seawater has a high concentration of sulfate, where they are responsible for up to 50% of carbon remineralization (*2*). Sulfate-reducing prokaryotes present a grave economic problem to the oil industry because of their involvement in biocorrosion and souring of oil and gas deposits (*3*, *4*). These organisms have also been implicated in inflammatory bowel diseases, because of the toxic effects of sulfide to colonic epithelial cells (*5*). On a positive side, sulfate-reducing organisms are important players in bioremediation of polluted environments (*6*), namely, in decontamination of toxic metals and radionuclides (*7*) or aromatic and chlorinated compounds (*8*).

Despite the widespread occurrence and the importance of sulfate reduction, the understanding of the energy conservation mechanisms of this anaerobic respiration is still in its infancy. The sulfate respiratory chain displays significant differences from other bacterial systems, because sulfate-reducing organisms lack important complexes such as complex I and the bc_1 complex. However, it has long been shown that sulfate reduction is associated with oxidative phosphorylation and that these organisms contain menaquinone, which is likely to be involved in the respiratory chain. Before being reduced, sulfate is transported to the cytoplasm where it is activated by a reaction with ATP to form adenosine 5′-phosphosulfate (APS).[1] APS is the first true electron acceptor and is reduced by APS reductase to sulfite, which is then reduced by the dissimilatory sulfite reductase, both soluble cytoplasmic enzymes. The electron donors to APS reductase and sulfite reductase are not known, but it is likely that the reducing equivalents will be transferred from the membrane menaquinone pool, certainly involving membrane redox proteins. Furthermore, one of the main energy sources for sulfate-reducing organisms, hydrogen, is oxidized

† This work was supported by FCT Grants POCTI/ESP/44782/2002 to I.A.C.P., POCTI/QUI/47866/2002 to A.V.X., and POCTI/BME/37406/2002 to M.T. R.H.P. was a recipient of the FCT Ph.D. Grant SFRH/BD/1324/2000.

* To whom correspondence should be addressed: ITQB, Av. da Republica, EAN, Apt. 127, 2781-901 Oeiras, Portugal. Telephone: 351-214469327. Fax: 351-214411277. Website: http://www.itqb.unl.pt. E-mail: ipereira@itqb.unl.pt.

[1] Abbreviations: APS, adenosine 5′-phosphosulfate; *Dd*27k, *Desulfovibrio desulfuricans* ATCC 27774; DM, *n*-dodecyl-*β*-D-maltoside; Hdr, heterodisulfide reductase; Hmc, high molecular mass cytochrome; HS-CoB, co-enzyme B; HS-CoM, co-enzyme M; TpIIc3, type-II cytochrome c_3; 9Hc, nine-heme cytochrome *c*; Qmo, quinone-interacting membrane-bound oxidoreductase complex.

10.1021/bi0515265 CCC: $33.50
Published on Web 12/13/2005

in the periplasm; therefore, electrons also have to go through the membrane (*9*).

Up until recently very little was known about membrane-associated proteins in sulfate-reducing organisms that could be involved in the respiratory mechanism, but this has changed in recent years. The first transmembrane redox complex to be identified at the gene level in sulfate-reducing organisms was the six-subunit Hmc complex of *Desulfovibrio vulgaris* Hildenborough (*10*), which is associated with a large periplasmic 16-heme cytochrome *c*, HmcA, whose structure was recently determined (*11*, *12*). Expression of this complex is higher in growth with H_2 (*13*), and studies with knock-out mutants (*14*, *15*) and, upon reduction of the cytochrome subunit (*16*), implicate it in electron transfer between periplasmic H_2 oxidation and the cytoplasm. This complex has not yet been isolated. A related but smaller complex was identified in *Desulfovibrio desulfuricans* ATCC 27774, which is associated with a nine-heme cytochrome (9HcA) (*17*). The structure of this cytochrome is similar to the C-terminal domain of the HmcA cytochrome (*18*). A simpler three-subunit complex was also identified in *D. vulgaris*, and this is associated with a tetraheme cytochrome named as type-II cytochrome c_3 ($TpIIc_3$) (*19*). The subunits of these three complexes have a strong amino acid sequence similarity between them, indicating they are homologous.

The first membrane redox complex to have been isolated from a sulfate-reducing organism was the Hme complex (for the Hdr-like menaquinol-oxidizing enzyme complex) from the sulfate-reducing archaeon *Archaeoglobus fulgidus* (*20*). This complex contains a subunit that is related to the catalytic subunit of heterodisulfide reductases (Hdr) from methanogens and is rapidly reduced by a menaquinol analogue, pointing to its involvement in the electron-transfer chain. The Hme complex is encoded in a five-gene operon, and the predicted proteins show similarity to proteins encoded in the *dsr* locus of the phototrophic sulfur bacterium *Allochromatium vinosum* (which also encodes subunits of the sulfite reductase) (*21*, *22*), as well as to the subunits of the Hmc complex.

Recently, another membrane redox complex of three subunits was isolated in our laboratory from *D. desulfuricans* ATCC 27774 and named as Qmo (*23*). Strikingly, all three subunits of the Qmo complex have homology to subunits of heterodisulfide reductases (HdrA, HdrC, and HdrE) from methanogens. Qmo has two FAD groups, two hemes *b*, and several FeS centers. Both hemes are reduced by a menaquinol analogue. The genes coding for Qmo are found adjacent to genes coding for the APS reductase in the genomes of several organisms, suggesting that Qmo may be involved in electron transfer from the quinone pool to APS reductase. In support of this idea, it was recently found that both sets of genes are downregulated in the presence of nitrite (*24*).

Similar to so many other areas, the advent of genomic information has greatly enhanced our understanding of respiratory pathways in sulfate-reducing prokaryotes. *A. fulgidus* was the first sulfate-reducing organism to have its genome sequenced (*25*), but recently the genomes of the soil bacterium *D. vulgaris* Hildenborough (*26*) and the marine psycrophilic bacterium *Desulfotalea psycrophila* (*27*) were also published. Genomic information is also available for another *Desulfovibrio* spp. (*D. desulfuricans* G20). *Desulfovibrio* are the most extensively studied organisms among the sulfate-reducing prokaryotes. Analysis of the *D. vulgaris* genome identified 177 gene products likely to be involved in energy metabolism (*28*), pointing to the existence of multiple respiratory pathways as is commonly observed in bacteria. Several transmembrane redox complexes can be identified in this organism, but a comparison with the genomes of the other sulfate-reducing organisms reveals that only two are strictly conserved, suggesting that these are the truly essential ones for sulfate reduction. They are the three-subunit Qmo complex and the five-subunit Dsr complex encoded by the *dsrMKJOP* genes in *Desulfovibrio* (*24*) and named Hme in *A. fulgidus*. As discussed above, Qmo is likely to be involved in electron transfer from the quinone pool to APS reductase, whereas the Dsr complex is probably involved in electron transfer to the sulfite reductase because its genes are part of a locus that includes the genes for sulfite reductase in several organisms, like *A. vinosum* (*21*, *22*) or *Chlorobium tepidum*, and in *A. vinosum*, proteins from the Dsr complex are co-purified with the sulfite reductase (*22*). Within a selection of genes predicted to encode proteins involved in energy metabolism, the Dsr genes were found among those most highly transcribed in *D. vulgaris* grown in lactate/sulfate (*28*). *Desulfovibrio* spp. are noteworthy in that they contain other membrane redox complexes related to Dsr, of which the most similar is the Hmc complex. However, no complex of this family has yet been isolated in *Desulfovibrio* spp.

After having isolated the Qmo complex from *D. desulfuricans* ATCC 27774 (*Dd*27k) (*23*), we set out to isolate the Dsr complex to further elucidate its role in the sulfate respiratory chain. We report here the isolation and detailed characterization of this complex from *D*d27k. The complex is encoded by the *dsrMKJOP* genes in the genomes of *D. vulgaris* and *D. desulfuricans* G20 and thus was named as the Dsr complex to agree with this nomenclature. The isolated Dsr complex includes a novel periplasmic triheme cytochrome *c* with unique characteristics, including a heme with unusual His/Cys ligation, and a cytoplasmic FeS protein, which displays a paramagnetic EPR signal in the oxidized state that is indicative of the presence of an unusual catalytic [4Fe−4S] center, also identified in Hme. The function of this complex in sulfate respiration is discussed within the context of the present genome data of sulfate-reducing organisms and the information thus far available on other membrane complexes thought to be involved in the respiratory metabolism of sulfur compounds.

MATERIALS AND METHODS

Bacterial Growth. Cells of *D*d27k were grown according to ref *23*. The cells were suspended in 10 mM Tris-HCl buffer at pH 7.6 and ruptured by passing twice through a Manton−Gaulin press. The resulting extract was centrifuged at 10000*g* for 15 min to remove cell debris, and the crude membrane fraction was obtained by centrifuging the supernatant at 100000*g* for 2 h.

Protein Purification. All purification steps were conducted aerobically in a cold cabinet at 6 °C. The crude membrane fraction from *D*d27k was washed by suspending in 20 mM Tris/HCl at pH 7.6 with 10% glycerol (v/v) and ultracentrifuging at 140000*g* for 2 h. The pellet obtained was solubilized in 50 mM Tris/HCl at pH 7.6 buffer containing 10% glycerol (v/v) and 4% (w/v) *n*-dodecyl-β-D-maltoside

(DM), in the presence of Complete protease inhibitor cocktail tablets (Roche Diagnostics GmbH, Germany). Solubilization was carried out for 1 h in an ice bath with gentle stirring. The solubilized protein was separated by ultracentrifugation at 140000*g* for 2 h, and the pellet was used for a second solubilization using the same conditions as described above. The total solubilized protein was applied to a DEAE column equilibrated with buffer A containing 50 mM Tris/HCl at pH 7.6, 10% glycerol (v/v), 0.1% (w/v) DM, and a quarter of a Complete tablet/L. A stepwise gradient of an increasing NaCl concentration was performed. Fractions were analyzed by UV−vis spectroscopy to search for the presence of both hemes *b* and *c* in the same sample. A fraction with such characteristics eluted at 300−400 mM NaCl and its ionic strength was lowered by dilution in buffer A. This fraction was then loaded on a Q-Sepharose column equilibrated with 50 mM Tris/HCl at pH 7.6 buffer containing 0.1% (w/v) DM and 10% glycerol (v/v). A stepwise gradient of an increasing NaCl concentration was performed, and the fraction eluted at around 350 mM NaCl was collected. Coomassie-blue stained SDS−PAGE typically revealed that these two steps provided a 90% pure Dsr complex. Whenever a fraction was judged impure, it was further purified by size-exclusion chromatography with a Superdex S200 column (Amersham Pharmacia Biotech) equilibrated with buffer A with 100 mM NaCl. After each chromatographic step, protein fractions were concentrated either in an Amicon ultrafiltration cell or in an Amicon Centriplus device using membranes with molecular cutoffs of 100 kDa.

Analytical Methods. The protein concentration was determined with the Bicinchoninic Acid assay from Pierce, using bovine serum albumin as the standard. For SDS gels, proteins were incubated with sample buffer for 30′ at room temperature before loading on the gel. For N-terminal sequencing, the subunits were separated by Tricine-SDS−PAGE and blotted to a PVDF membrane (Millipore) using a Trans-Blot SD semidry electrophoretic transfer cell (Bio-Rad). Sequencing was conducted in an Applied Biosystems 491 HT sequencer. The pyridine hemochrome derivative was prepared as described earlier (*29*). Hemes were extracted from the protein and analyzed by reverse-phase chromatography as described in ref *30*. Nonheme iron was determined by the 2,4,6-Tris(2-pyridyl)-*s*-triazine method (*31*).

Interaction Experiments: Menadiol−Dsr. Menadione was purchased from Sigma and reduced to menadiol in an anaerobic chamber (95% N_2, 5% H_2) with sodium borohydride (*32*). Monitoring the reduction process spectrophotometrically, borohydride was added stepwise until full reduction occurred. Menadiol was added to the Dsr protein solution (0.4 mg/mL) in the anaerobic chamber up to the final concentration of 1 mM. Spectra were recorded in a Shimadzu UV-1203 spectrophotometer. After 5 min, an excess of sodium borohydride was added to ensure that menadione was in a fully reduced form and spectra were recorded again. To achieve maximal protein reduction, an excess of sodium dithionite was then added. As a control experiment, the same protein solution was reduced with an identical excess of sodium borohydride, in the absence of menadiol.

[NiFe] Hydrogenase−Dsr. The experimental setup and conditions are identical to a previously published report (*19*). Hydrogenase was added in different concentrations (30 nM and 1.41 μM) to 1.0 mg/mL of Dsr, in the absence and presence of catalytic quantities (30 nM) of cytochromes c_3 and c_{553}.

Spectroscopic Methods. Room-temperature UV−visible spectra were obtained using a Shimadzu UV-1603 spectrophotometer. Liquid nitrogen temperature spectra were obtained in an OLIS DW-2 instrument. EPR spectra were recorded using a Brucker ESP 380 spectrometer equipped with an ESR 900 continuous-flow helium cryostat from Oxford Instruments, as described before (*23*). For relative spin quantitations, the EPR signals were theoretically simulated, and the intensity of each simulation was compared with the experimental data.

Redox Titration. Redox titrations monitored by visible spectroscopy were performed in an anaerobic chamber in 100 mM Tris/HCl buffer at pH 7.6, following the changes in absorbance at the Soret band of the reduced hemes, corrected for the corresponding isosbestic points, and using buffered sodium dithionite as the reductant. The following redox mediators were used (at a final concentration of 0.8 μM each): 1,2-naphthoquinone, phenazine methosulfate, phenazine ethosulfate, methylene blue, indigo tetrasulfonate, indigo trisulfonate, indigo disulfonate, 2-hydroxy-1,4-naphthoquinone, Safranine, neutral red, benzyl viologen, and methyl viologen. The reduction potentials were measured with a combined Ag/AgCl electrode calibrated against a saturated quinhydrone solution at pH 7 and are referenced to the standard hydrogen electrode.

Sequence Analysis Tools. Blast searches were performed at the NCBI website (http://www.ncbi.nlm.nih.gov/BLAST/). Sequence data were retrieved and analyzed at The Institute for Genomic Research website (http://www.tigr.org), the DOE Joint Genome Institute website (http://www.jgi.doe.gov/JGI_microbial/html/index.html), and the VIMSS Comparative Genomics website (http://www.microbesonline.org/). Multiple alignments were performed using CLUSTALX. Sequence analysis and transmembrane helix predictions were done using programs available at http://us.expasy.org/.

RESULTS

Purification and Biochemical Characterization of the Dd27k Dsr Complex. Membrane proteins of *Dd*27k were solubilized using the detergent dodecyl-β-D-maltoside. The detergent extract was initially purified on a DEAE anionic exchange column, from which an acidic heme-containing fraction was identified. This fraction was further purified on Q-Sepharose and Superdex 200 columns. The protein thus obtained displayed four bands on a SDS gel (Figure 1A) with apparent molecular masses of 60, 38, 27, and 15 kDa. The 15-kDa polypeptide was positively identified as a *c*-type cytochrome by heme-staining (data not shown). N-Terminal sequences were obtained for the 60- and 27-kDa bands, whereas the 38- and 15-kDa bands gave no sequence possibly because of blocked N terminals. The two sequences obtained were used to search the genome of *D. vulgaris* for the corresponding genes, which enabled their identification as genes DVU1289 (60-kDa band) and DVU1287 (27-kDa band) (Table 1), which are part of the predicted five-gene operon encoding the Dsr complex (*33*). In *D. vulgaris*, the *dsrMKJOP* operon (genes DVU1286−DVU1290) codes for proteins with 61 kDa (DVU1289; DsrK), 43 kDa (DVU1286; DsrP), 38 kDa (DVU1290; DsrM), 29 kDa (DVU1287;

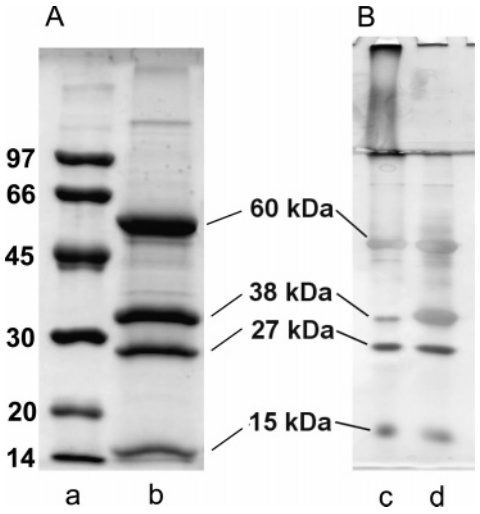

FIGURE 1: SDS−PAGE of the *Dd*27k Dsr complex (A) stained with Coomassie Blue and (B) stained with silver. (a) Molecular mass markers, (b) Dsr complex incubated in loading buffer without β-mercaptoethanol (20 μg), (c) Dsr complex incubated in loading buffer with β-mercaptoethanol (5 μg), and (d) without it.

DsrO), and 15 kDa (DVU1288; DsrJ). The gene DVU1286 codes for a highly hydrophobic protein of 43 kDa (DsrP), which is not apparent in the SDS−PAGE of the isolated complex. This protein probably does not run on the gel because of protein aggregation, a common effect with very hydrophobic proteins. A similar result was observed for the Hme complex from *Archaeoglobus fulgidus* (*20*). Attempts to solubilize this protein with a double amount of SDS or with 8 M urea in the sample buffer were unsuccessful. Evidence of protein aggregation is apparent in silver-stained gels, where a protein band is observed at the top of the stacking gel, along with a smeared protein pattern down to the resolving gel (Figure 1B). When β-mercaptoethanol is not present in the sample buffer, the smeared pattern is not observed, indicating an increase in the solubilized material. With this treatment, the intensity of the 38-kDa band increases significantly and a faint band that could be due to the 43-kDa protein appears. However, a protein band is still observed at the top of the stacking gel.

Desulfovibrio DsrMKJOP-Encoded Proteins. The operon coding for the Dsr complex is present in the genomes of all sulfate-reducing organisms sequenced to date. In *D. vulgaris* Hildenborough, *D. desulfuricans* G20, and *Desulfotalea psycrophila* this operon has the same gene organization (*dsrMKJOP*), whereas in *A. fulgidus*, it is *dsrOPMKJ* (*20*) (Figure 2). The characteristics of the *Dd*27k Dsr complex presented here strongly indicate that in this organism the *dsr* operon is identical to that found in the genomes of all sulfate-reducing organisms sequenced. In two bacteria that do not reduce sulfate, the acetogenic bacterium *Moorella thermoacetica* (reduces thiosulfate) and the dehalogenating bacterium *Desulfitobacterium hafniense* (reduces sulfite), a very similar Dsr complex is encoded in the same locus as the *dsrAB* genes coding for the catalytic and electron-transferring subunits of the dissimilatory sulfite reductase. Strikingly, both the sulfite reductase and the Dsr complex are also found in organisms performing the opposite type of metabolism to sulfate-reducing organisms, that is oxidizing reduced sulfur compounds as energy sources, like the phototrophs *A. vinosum* and *C. tepidum* or the chemotroph *Thiobacillus denitrificans*. In these three organisms, the *dsrMKJOP* genes are also part of the same locus as the *dsrAB* genes (*21*, *22*).

The *Desulfovibrio* DsrMKJOP proteins show the highest amino acid sequence identity to the other Dsr proteins found in genomes sequenced to date (see the Supporting Information), which belong to the organisms depicted in Figure 2. A sequence analysis of the DsrMKJOP proteins from *A. fulgidus* and *A. vinosum* has been presented before (*20*−*22*), but some further details are highlighted here. The DsrM proteins (38 kDa) belong to the family of integral membrane subunits of respiratory oxido-reductases that bind two hemes *b* on opposite sides of the bilayer and are responsible for electron transfer across the membrane, which may be associated with the generation of a proton gradient (*34*). The *Desulfovibrio* DsrM is predicted to contain six transmembrane helices and has five histidines, strictly conserved in other DsrM proteins, four of which are likely candidates to bind two hemes *b*. These four histidines align with the histidines that are the ligands to the two hemes *b* in *Escherichia coli Nar*I (*35*). However, in DsrM, the last of these histidines is not predicted to be located in a transmembrane helix, in contrast to *Nar*I, where two transmembrane helices contain the four histidine ligands.

DsrK is predicted to be a cytoplasmic iron−sulfur protein (61 kDa) that is related to the cytoplasmic catalytic subunit HdrD of membrane-bound heterodisulfide reductases from methanogenic archaea (*36*). The DsrK proteins contain two $[4Fe-4S]^{2+/1+}$ binding sites as HdrD but only one of the five-cysteine motifs, $CX_nCCX_nCX_2C$, of which HdrD has two. These five-cysteine motifs are also found in subunits of several other proteins including type E succinate:quinone oxidoreductase (SdhE), thiol:fumarate reductase (TrfB), the *Desulfovibrio* Hmc complex (HmcF), glycolate oxidase (GlcF), and anaerobic glycerol-3-phosphate dehydrogenase (GlpC) (*37*, *38*). In HdrD, some of these cysteines are involved in the binding of a [4Fe−4S] cluster that is the catalytic site for reduction of the heterodisulfide (*39*−*43*). One interesting point is that in DsrK from several organisms (*Desulfovibrio*, *D. psycrophila*, *D. hafniense*, *A. fulgidus*, *M. thermoacetica*, and *C. tepidum*) the last cysteine of the $CX_nCCX_nCX_2C$ motif is replaced by a conserved aspartate, whereas in DsrK from *A. vinosum*, *T. denitrificans*, *Magnetococcus* MC-1, or *Magnetospirillum magnetotaticum* the cysteine is conserved (see the Supporting Information). This may suggest that only the first four cysteines of the motif are involved in cluster binding, but it cannot be ruled out that the aspartate may also be a ligand to the [4Fe−4S] center.

The DsrJ protein (15 kDa) contains three, closely spaced, heme *c* binding sites (CXXCH) at the C terminus and an N-terminal signal sequence for export to the periplasm by the Sec pathway (*44*). This signal peptide is not cleaved off in the corresponding protein of the *A. fulgidus* Hme complex (*20*) and probably serves as a membrane anchor for the periplasmic cytochrome. The DsrJ sequence shows no homology to other cytochromes in the databases and therefore corresponds to a novel family of cytochromes *c*. In particular, it shows no relationship to the family of cytochromes c_3, so abundant in *Desulfovibrio* organisms, including HmcA and the type-II cytochrome c_3, which are both also associated with transmembrane redox complexes

Table 1: Alignment of N-terminal Sequences of the 60 KDa and 27 KDa Bands with the N-terminal Sequences of *D. Vulgaris* Hildenborough Genes Showing Highest Sequence Identity

60 kDa band **DsrK (DVU1289)**	-AKLPTPQMLVASRPDFPAEDWLDVKPFETPG |||||: |:||:| |||| | |||| || MSKLPTPEQLIASKPGFPAESWMDVKPDFRPG	62% identity; 78% similarity
27 kDa band **DsrO (DVU1287)**	QIAPGKYERAANALHAKRWGMVIDTRQFKGPEDYKPKIEAAHHS |||| | || |||| |||| |:| |||| ||| | AALTGKYEDGATALKAKRWAMVIDMRKFTSPEDYSRVIEACHSI	56% identity; 59% similarity

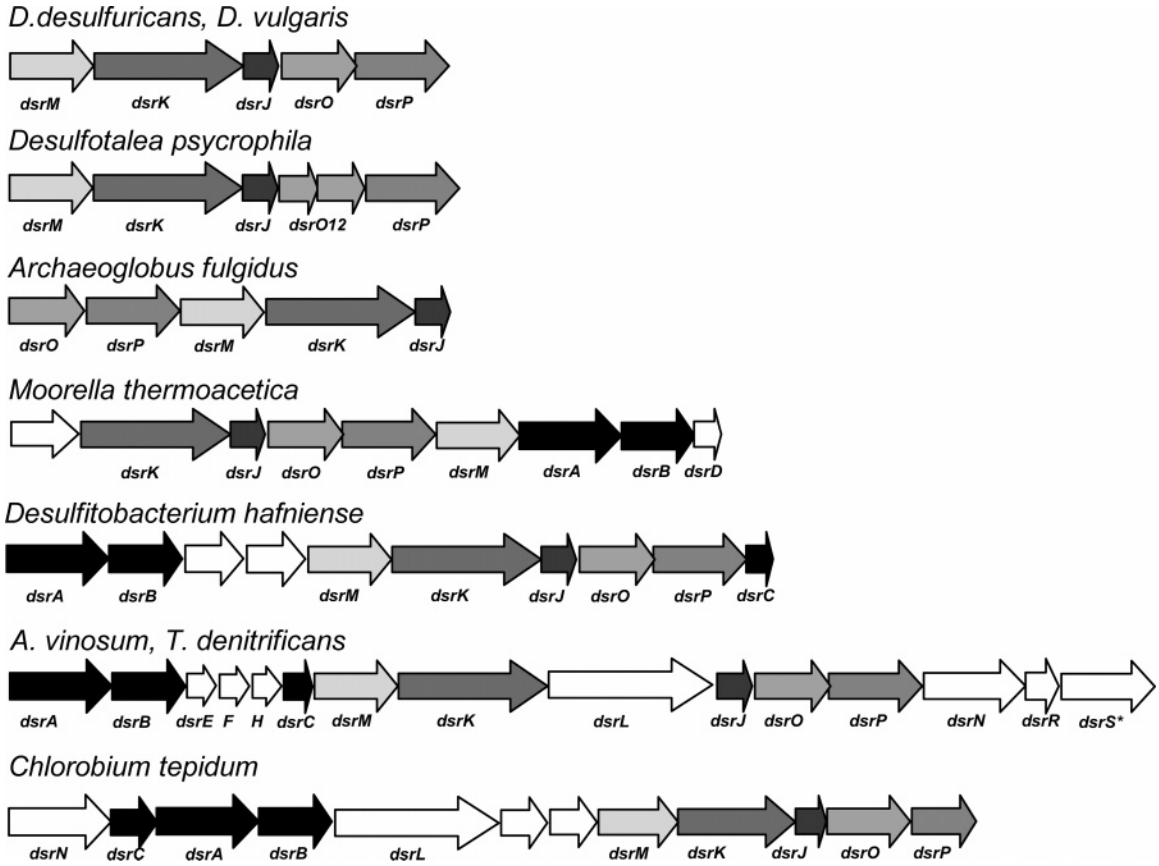

FIGURE 2: Schematic representation of the genes encoding the Dsr complex in several organisms. The genes represented correspond to genes DVU1290−DVU1286 of *D. vulgaris* Hildenborough, Dpsy4178−Dpsy4172 for *Desulfotalea psycrophila*, AF499−AF503 for *Archaeoglobus fulgidus*, and CT2251−CT2240 for *Chlorobium tepidum*. Genes for the other organisms are from preliminary genome data; therefore, gene numbers are still not attributed. The *dsrMKJOP* genes are in shades of gray; the *dsrABC* genes are in black; and other genes are in white. (*) The *dsrS* gene is not found in *T. denitrificans*.

(*9*). In cytochromes *c*, the histidine of the CX_2CH heme-binding site is invariably found to coordinate the iron of that heme. Thus, the three hemes in DsrJ will have at least one histidine ligand. Analysis of a sequence alignment of DsrJ proteins (see the Supporting Information) indicates that there are not enough histidines for all of the hemes to have the bis-His ligation that is common for multiheme cytochromes *c* (*45*). There are four conserved residues that may serve as the sixth ligands to the three hemes: two methionines, one cysteine, and one histidine. However, one of the methionines is not conserved in one case (DsrJ from *Magnetospirillum magnetotaticum*), suggesting that it is probably not a ligand to a heme because these residues are usually strictly conserved in homologous cytochromes (see further analysis below).

The DsrO protein is a periplasmic FeS protein that belongs to the family of ferredoxin-like electron-transferring subunits found in several respiratory membrane-associated enzymes. The DsrO proteins include a typical signal peptide for translocation to the periplasm via the Tat pathway (*46*), which is cleaved off because it is not detected in the mature protein. Most of the DsrO proteins (and other proteins in this family) contain typical binding sites for four [4Fe−4S]$^{2+/1+}$ centers, but the DsrO from *D. vulgaris*, *D. desulfuricans* G20, *D. psycrophila*, and *D. hafniense* are different in that they are missing the first [4Fe−4S]$^{2+/1+}$ binding site (with exception of the last cysteine of the binding site, which is conserved) and also the last cysteine of the fourth [4Fe−4S]$^{2+/1+}$ binding site. This could indicate that this last center is of the [3Fe−4S]$^{+1/0}$ type, but there is no evidence for this by EPR (see below); therefore, either this center is not present or a different residue is serving as a ligand for a [4Fe−4S]$^{2+/1+}$ center, including possibly the cysteine that is the only conserved residue from the missing first [4Fe−4S]$^{2+/1+}$

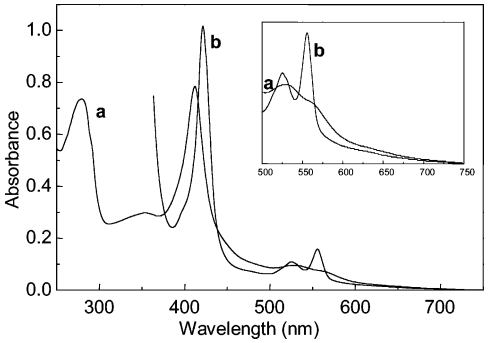

FIGURE 3: UV/vis spectrum of the isolated *Dd*27k Dsr complex in the oxidized (a) and reduced (b) form. The inset is a close-up view of the 750−500 nm region.

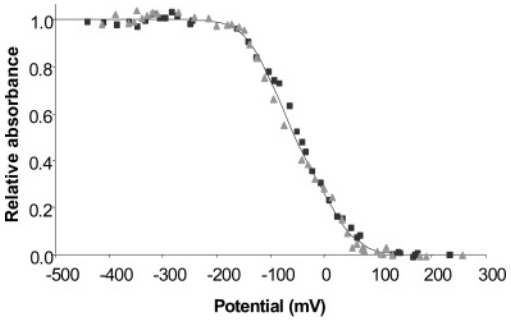

FIGURE 4: Redox titration of Dsr hemes followed by UV/visible spectroscopy. The points represent reduction (■) and oxidation (▲) of Dsr following the Soret band at 421.5 nm. The full line corresponds to a theoretical simulation obtained by adding three Nernst equations with redox potentials of +20, −60, and −110 mV.

center. Also, in *D. vulgaris*, *D. desulfuricans* G20, and *D. hafniense*, a serine is replacing the missing cysteine and could act as fourth ligand to the center. In the *D. psycrophila* DsrO, a serine is also found three residues away. DsrO from *D. psycrophila* is unique in that it is encoded by two adjacent genes, one coding for the N-terminal part and including the Tat signal peptide and the other encoding the C-terminal region including the $[4Fe-4S]^{2+/1+}$ clusters. There are no predicted transmembrane helices in the DsrO proteins, in contrast to the corresponding proteins from the *Desulfovibrio* Hmc and 9Hc complexes (HmcB and 9HcB), which are predicted to contain a transmembrane helix and a cytoplasmic-facing domain at the C terminus (*17*, *47*).

DsrP is an integral membrane protein predicted to contain 10 transmembrane helices. It is related to the membrane subunit of *E. coli* hydrogenase-2 (HybB), which acts as a menaquinone reductase and possibly binds heme *b* (*48*). There are some conserved histidines among a number of the DsrP proteins but not all of them, and the predicted position of these histidines relative to the transmembrane helices is not suggestive of their involvement in heme binding. Furthermore, when DsrO proteins are aligned with other proteins in this family, no conserved histidines are found. Thus, at this point, there is no clear evidence to indicate that any of the proteins in this family bind hemes *b*. One of these histidines (H_{176} of *D. vulgaris* DsrP) is possibly part of a quinone-binding site of the type AX_3HX_2T (*49*) that is conserved in several but not all DsrP proteins.

UV−Visible Spectroscopy. The *Dd*27k Dsr complex has a strong absorbance in the visible region as expected from a protein containing several hemes and FeS centers (Figure 3). In the oxidized spectrum, a heme Soret peak is observed at 412 nm and there is also a broad, weak absorption between 600 and 700 nm that can be attributed to a His/Met-bound heme (and to the small amount of high-spin heme detected by EPR). In the reduced state, the Soret peak shifts to 421.5 nm and the heme α and *β* peaks are observed at 555.5 and 525 nm, respectively. The α peak is quite broad in agreement with the presence of both *b*- and *c*-type hemes, and this is more apparent in a low-temperature spectrum, although two separate peaks cannot be resolved (data not shown). Non-covalently bound hemes were extracted with acetone/HCl, and their pyridine hemochrome spectrum displayed an α peak at 555.5 nm, confirming these as standard *b*-type hemes. This result was verified by HPLC identification of the extracted hemes, which present a similar retention time to protoheme IX extracted from hemoglobin. In the homologous Hme complex from *A. fulgidus*, the pyridine hemochrome of the extracted heme displayed blue-shifted values for the α and *β* bands, relative to protoheme IX, suggesting the presence of a modified heme in this complex, and this was also observed for an HmeCD complex from *A. profundus* (*50*). This is not the case in *Dd*27k Dsr, which contains heme(s) *b*.

Sequence analysis of the Dsr complex predicts the presence of three hemes *c* (in DsrJ) and two hemes *b* (in DsrM), if these subunits are present in a 1:1 ratio in the complex. In several preparations obtained for the Dsr complex, we always observed an excess of hemes *c* versus hemes *b*, in contrast to the case of Hme from *A. fulgidus*, where the 16-kDa cytochrome *c* was present in substoichiometric amounts and was even absent in some preparations. We estimated the concentration of hemes *b* and *c* in the Dsr complex using the method described by Berry and Trumpower (*29*) and observed a ratio of 1.8 of hemes *c*/hemes *b*, which is close to the predicted value of 1.5. However, we did observe some variation in this ratio from batch to batch, which increases with a higher number of purification steps, suggesting the loss of the cytochrome *b* membrane subunit but not the cytochrome *c* subunit. With careful peak selection during chromatography, it was possible to obtain a fairly pure Dsr complex in two steps, which displayed a heme *c*/heme *b* ratio close to the predicted value of 1.5.

A redox titration monitored by visible spectroscopy was performed to estimate the reduction potential of the hemes, following changes at the Soret band. It was observed that the maximum value or shape of the α band did not shift during the titration. The hemes start to be reduced at ∼ +100 mV and are fully reduced at ∼ −200 mV (Figure 4). The experimental points could be simulated by adding a minimum of three Nernst equations with redox potentials of +20, −60, and −110 mV in a 1:1:1 ratio. We did not attempt to attribute redox potentials to individual hemes for the following reasons: (i) there are different types of hemes (*b* and *c*) with distinct coordinations that will therefore contribute differently to the absorbance at any given wavelength; (ii) one of the hemes is not fully reduced with dithionite as shown by EPR (see below); (iii) it is likely that there is redox cooperativity between the hemes and possibly the FeS centers, as commonly observed in multiredox center proteins (*45*), which affect the macroscopic redox potentials determined in the redox titration.

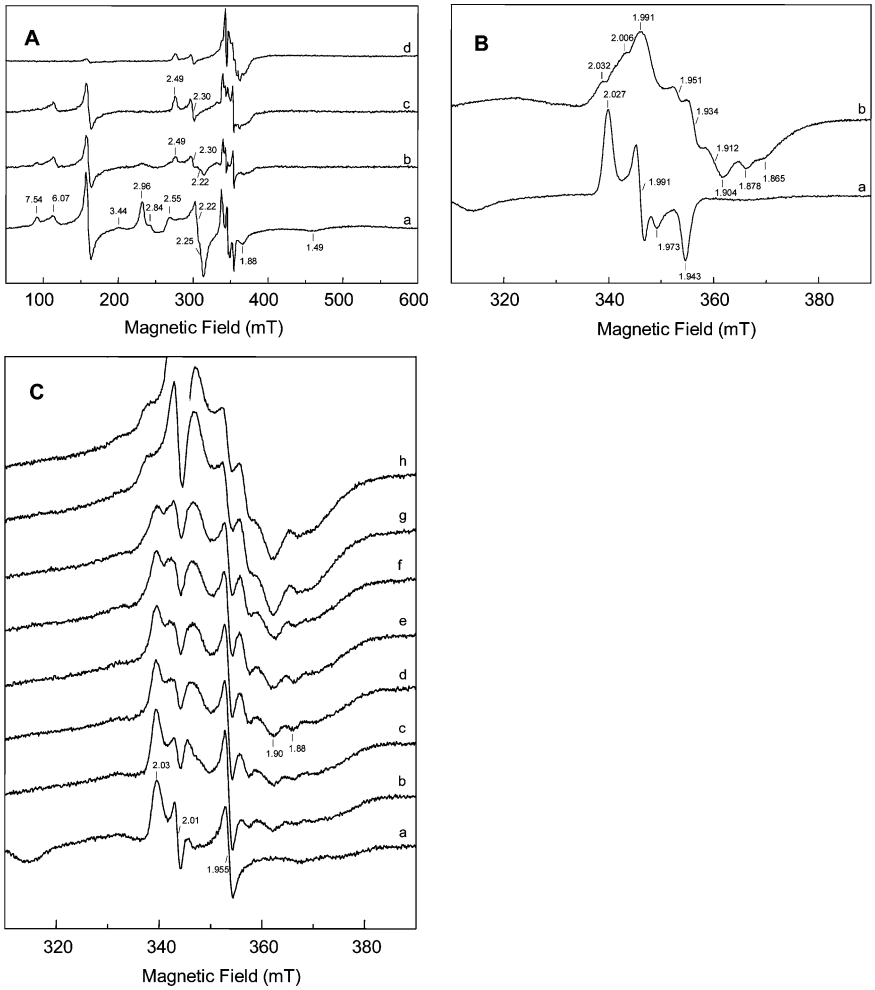

FIGURE 5: EPR spectra of the *Dd*27k Dsr complex. (A) (a) Fully oxidized. (b−d) Spectra taken during the redox titration: (b) at +2 mV, (c) at −36 mV, and (d) at −400 mV; (B) (a) Fully oxidized. (b) Reduced with dithionite. (C) Spectra taken during the redox tritration: (a) +2 mV, (b) −36 mV, (c) −78 mV, (d) −119 mV, (e) −154 mV, (f) −196 mV, (g) −246 mV, and (h) −294 mV. Experimental conditions: microwave frequency, 9.64 GHz; microwave power, 2.4 mW; modulation frequency, 100 kHz; and modulation amplitude, 1 mT. Temperature of 10 K for all spectra except for spectrum B (a) (15 K).

Table 2: Assignment of the Most Relevant EPR Signals Observed in the *Dd*27k Dsr Complex

g_{max}	g_{med}	g_{min}	detected in oxidized form	detected in reduced form	assignment
2.96	2.25	∼1.5	+	−	bis-His bound hemes
2.84	na[a]	na[a]	+	−	histidinate-bound heme
3.44	na[a]	na[a]	+	−	His-Met bound heme
∼2.55	2.22	1.88	+	−	His-Cys$^-$ bound heme
2.487	2.297	na[a]	−	+	His-Cys$^-$ bound heme
2.027	1.994	1.943	+	−	[4Fe−4S]$^{3+}$ center
2.03−1.86			−	+	[4Fe−4S]$^{2+/1+}$ centers

[a] na = not assigned.

EPR Spectroscopy. EPR spectroscopy of the as-prepared Dsr complex exhibits an interesting and complex set of features (Figure 5A, a), which are unaltered upon further oxidation with iridium(IV) chloride. A summary of the most relevant EPR signals is presented in Table 2. The EPR spectrum is dominated by an intense rhombic signal with $g_{max} = 2.027$, $g_{med} = 1.994$, and $g_{min} = 1.943$ (Figure 5B, a), which shows the highest intensity at temperatures of 15−17 K and broadens beyond detection at temperatures higher than 50 K. The spin intensity of the $g_{max} = 2.027$ signal is about 10% of that of the species with $g_{max} = 2.96$, which corresponds to two hemes (see below), suggesting that the signal is present in 20% of the molecules. The $g_{max} = 2.027$ signal is very similar to that displayed by Hme from *A. fulgidus* (*20*) and *A. profundus* (*50*) and also to a signal observed in heterodisulfide reductases (Hdr) upon addition of one of the thiol substrates to the oxidized enzyme (*39*, *40*). In Hdr, this rhombic signal is attributed to a [4Fe−4S]$^{3+}$ cluster formed by direct binding of the thiolate substrate to a [4Fe−4S]$^{2+}$ cluster, which is believed to be the active site of the enzyme (*40*−*43*). This active-site [4Fe−4S] cluster of Hdr is thought to be bound by the cysteines of two conserved five-cysteine motifs ($CX_nCCX_nCX_2C$) found in HdrB of HdrABC and HdrD of HdrED (*37*). The DsrK proteins contain only one such motif, which presumably binds a [4Fe−4S] cluster that is responsible for the paramagnetic species observed in the oxidized Dsr complex. No signal because of a [3Fe−4S]$^{+1/0}$ center is observed in the oxidized Dsr enzyme, ruling out the presence of such a type of center in the periplasmic DsrO subunit.

The EPR spectrum of the Dsr complex is very informative regarding the coordination of the hemes *c* present (Figure 5A). It shows features typical of low-spin hemes, with the strongest signal having *g* values of 2.96, 2.25, and ∼1.5, which may be attributed to bis-histidine or bis-methionine

bound hemes. A smaller overlapping signal has a g_{max} = 2.84 that is suggestive of an histidinate-bound low-spin heme. A low-intensity resonance observed at g = 3.44 is characteristic of low-spin ferric hemes in a quasi-axial ligand field; the other two resonances of such a species are generally very broad and difficult to detect. The three signals with g_{max} of 3.44, 2.96, and 2.84 were simulated to estimate the relative amounts of the corresponding hemes, resulting in a ratio of ~1:2:1, respectively. In addition, the EPR spectrum displays a broad absorption resonance that shows one distinct g_{max} at 2.55. Such a low g_{max} value is uncommon but is observed in hemes *b* with cysteinate coordination distal to a nitrogenous ligand as in the CO-sensor CooA (Cys^-/Pro in the oxidized state) (*51*, *52*) or cystathionine β-synthase (*53*) and in nitrogenous derivatives of cysteinate-bound heme proteins (*54*), like cytochrome P-450 (*55*) and endothelial NO synthase (*56*). Thiolate ligation in a heme *c* is very unusual with only two cases reported to date. They are the 32-kDa SoxA subunit of the SoxAX complex involved in thiosulfate oxidation (*57*), for which EPR spectra have been reported for the proteins isolated from *Rhodovulum sulfidophilum* (*54*), *Starkeya novella* (*58*), and previously from *Paracoccus versutus* (*59*), and the 40-kDa triheme cytochrome PufC bound to the photosynthetic reaction center (*60*). Neither of these cytochromes bears any sequence similarity to DsrJ. The *R. sulfidophilum* SoxA contains two hemes with nitrogenous/thiolate ligation, of which one has His/Cys^- coordination, and the other, considered to be the active site, has a histidine and a cysteine persulfide as ligands (*61*). The EPR spectrum of SoxAX displays two signals LS_1 (g = ~2.55, 2.30, and ~1.87) and LS_2 (g = 2.42, 2.25, and 1.92) attributed to the thiolate-bound hemes (*54*). The LS_1 signal shows some heterogeneity and can be simulated with two components, LS_{1a} (g = 2.582, 2.301, and 1.868) and LS_{1b} (g = 2.524, 2.231, and 1.840). It is proposed that both hemes contribute to the LS_1 resonance, whereas the LS_2 resonance is attributed to the modified heme only. This is confirmed in the *S. novella* SoxAX cytochrome, which contains only the catalytic heme with the modified thiolate ligand but presents the same three resonances (*58*). In the *R. sulfidophilum* triheme cytochrome PufC, one of the hemes has His/Cys coordination and gives rise to resonances with g = 2.63, 2.26, and 1.79, because these are absent in the mutant where the cysteine ligand is replaced by a methionine (*60*). The g_{max} ~ 2.55 resonance observed in the *Dd*27k DsrJ is most likely due to a His/Cys^- bound heme, and this is supported by the sequence alignments of the DsrJ proteins, which show a strictly conserved cysteine (see the Supporting Information) as a likely candidate to be a heme ligand. The broad shape of this signal may be due to the presence of several possible conformations for this heme, as observed for SoxAX, or the presence of magnetic interactions between the paramagnetic centers. The other components of this signal are probably at g_{med} = 2.22 and g_{min} = 1.88. There is another g_{min} signal at g = 1.973 that we cannot attribute (Figure 5B, a). It may possibly correspond to a g_{min} of a different form of the thiolate-bound heme or another form of the paramagnetic species that originates the g_{max} = 2.027 rhombic signal. In *Methanothermobacter marburgensis*, the Hdr originates different forms of a $[4Fe-4S]^{3+}$ paramagnetic species upon incubation with either of its thiol products (HS-CoM and HS-CoB) in the oxidized form or with the disulfide substrate (CoM-S-S-CoB) in the reduced form (*39*). These three different signals differ particularly in their g_{min} value. Thus, on the basis of the EPR and sequence analysis, we propose that the two hemes *b* and one of the hemes *c* have bis-His coordination, a second heme *c* has His/Met coordination, and the third heme *c* has His/Cys coordination.

A redox cycled sample (dithionite-reduced and air-oxidized) of the *Dd*27k Dsr complex displays an EPR spectrum identical to the as-isolated, oxidized sample. In addition to the resonances discussed, the EPR spectrum shows also two weak high-spin signals at g = 6.07 and g = 7.54. The first is probably due to some His-bound high spin heme, whereas the second may originate from Cys-bound high-spin heme because it is similar to that observed for the high-spin form of cytochrome $P450_{cam}$ (*62*, *63*) and NO synthase (*56*). However, these resonances have a very low intensity compared to that of the low-spin hemes.

Upon reduction with sodium dithionite, the rhombic signal with g_{max} = 2.027 disappears and is replaced by a complex signal in the g ~ 2 region (Figure 5B, b), which is indicative of the presence of several reduced $[4Fe-4S]^{2+/1+}$ centers as predicted by sequence analysis. The line shape and g values observed indicate that there are multiple magnetic interactions between these centers. A redox titration followed by EPR was performed to try to further deconvolute the complex set of EPR signals. The rhombic signal with g_{max} = 2.027 was followed at 15 K and titrates with a midpoint redox potential of +130 mV considering a one electron-transfer reaction (data not shown). As this signal is reduced, another signal with a very similar g_{max} = 2.03, caused by a $[4Fe-4S]^{1+}$ center, starts to develop and is well-visible at 0 mV and both at 15 and 10 K (Figure 5C, a). The titration of the $[4Fe-4S]^{2+/1+}$ centers was followed at 10 K (Figure 5C). When subtractions of spectra taken along the titration are performed, it is possible to observe up to five different g_{max} resonances. The $[4Fe-4S]^{2+/1+}$ centers are reduced in a range of potentials between 0 and −300 mV.

In regard to the heme signals, the first to disappear is that at g = 3.42, which suggests that it corresponds to the His/Met bound heme, because these hemes commonly display higher redox potentials. The hemes corresponding to the signal at 2.96 are reduced next, and as this signal disappears, the broad resonance at g ~ 2.55 decreases and a new signal starts to develop with g_{max} = 2.487 and g_{med} = 2.297 (Figure 5A, b). As the potential decreases further, the 2.96 signal and the broad resonance disappear and only the 2.487 signal remains (Figure 5A, c). At this redox potential, the intensity of the 2.487 signal is roughly 50% of the 2.96 signal in the oxidized form, which correlates well with the first signal corresponding to one heme and the second to two hemes. The characteristics of the 2.487 signal indicate that it most likely also corresponds to the His/Cys bound heme, and this behavior suggests that reduction of one or several of the other hemes induces an alteration of the His/Cys bound heme, causing its heterogeneity to disappear and generating a simple signal. In the *R. sulfidophilum* purified reaction center, a signal at g_{max} = 2.47 was observed besides the g_{max} = 2.63 signal. The g_{max} = 2.47 signal is not observed in intact membrane fragments and was attributed also to the His/Cys-bound heme of the PufC cytochrome (*60*). The authors propose that the g_{max} = 2.63 to g_{max} = 2.47 transition corresponds to a relief of steric constraints on the conforma-

tion of the two heme ligands, and a similar situation may occur for the His/Cys-bound heme upon reduction of the Dsr complex. This heme is either redox-inactive or has an extremely low redox potential as the $g_{max} = 2.487$ signal is still observed at potentials of −400 mV, although its intensity decreases to about half below −250 mV but stays constant after that. A similar situation was observed for the His/Cys heme of *R. sulfidophilum* SoxAX, a fraction of which remains ferric in the presence of dithionite (*54*). The His/Cys bound heme of *R. sulfidophilum* PufC has a redox potential of −160 mV (*60*).

Functional Analysis of the Dsr Complex. The subunit arrangement of the Dsr complex suggests that it may interact with redox partners in the periplasm (through the cytochrome subunit DsrJ and the FeS subunit DsrO), with the membrane-associated menaquinone (through the membrane subunits DsrM and DsrP) or with redox partners in the cytoplasm (through the FeS subunit DsrK). We carried out some experiments to try to evaluate these possibilities. We tested the interaction with menaquinone by treating the Dsr complex with borohydride-reduced menadione (a menaquinone analogue) in an anaerobic chamber. This resulted in reduction of 40% of the hemes as compared to a dithionite-reduced sample. Because the Dsr sample used had a heme *b*/heme *c* ratio close to a 2:3 proportion, this suggests that the menadiol is able to reduce the hemes *b* of the membrane subunit DsrM but not all hemes in Dsr, which is also in agreement with the redox potentials determined. Treatment of the Dsr complex with $NaBH_4$ under identical conditions led to negligible heme reduction.

The cytochrome subunits, HmcA and TpIIc_3, that are also associated with two membrane redox complexes in *Desulfovibrio*, have been shown to be reduced by periplasmic-facing hydrogenases with the abundant tetraheme cytochrome c_3 (TpIc_3) as the mediator (*16*, *19*). We tested whether the Dsr complex could be reduced by the [NiFe] hydrogenase of *Dd*27k directly or in the presence of catalytic amounts of the *Dd*27k TpIc_3 or cytochrome c_{553}. No reduction of the Dsr hemes was observed in any situation, indicating that the hydrogenase or the cytochromes tested are not electron donors to the Dsr complex. This is in line with the fact that the DsrJ cytochrome is completely different from the HmcA and TpIIc_3, which belong to the cytochrome c_3 family (*45*). The presence of a His/Cys-bound heme *c* in DsrJ is very striking because this is such an unusual coordination for a heme *c*. Because this is observed also in SoxAX, a protein involved in thiosulfate oxidation in phototrophic and chemotrophic sulfur bacteria (*57*), we tested also whether several sulfur compounds (thiosulfate, tetrathionate, sulfite, and sulfide) affected the UV−vis spectrum of the oxidized or reduced Dsr. No effect was observed apart from some reduction of the hemes by sulfide, which is expected because of the difference in redox potentials.

DISCUSSION

In this study, we report the characterization of the Dsr complex from *Dd*27k, a complex proposed to be involved in the sulfate respiratory pathway. The Dsr complex was isolated from the membrane fraction of *Dd*27k and displays four subunits in a SDS gel with molecular masses of 60, 38, 27, and 15 kDa. The 15-kDa subunit was identified as a cytochrome *c* (DsrJ) by heme staining, and the N-terminal sequence of the 60- and 27-kDa bands permitted its identification as the DsrK and DsrO proteins, respectively, from the genomes of the closely related organisms *D. vulgaris* Hildenborough and *D. desulfuricans* G20. The genes encoding these proteins are part of a five-gene cluster, *dsrMKJOP*, which is predicted to form an operon in the genomes of all sulfate-reducing organisms sequenced to date (*33*). The 38-kDa band can be attributed to the heme-*b*-containing protein DsrM, whereas the integral membrane protein DsrP is not detected by SDS gel. The UV−vis and EPR spectra of the Dsr complex confirms the presence of the sequence-based predicted redox centers including several FeS centers, hemes *c*, and hemes *b*.

A homologue of the *Dd*27k Dsr complex, named Hme, has been isolated from the sulfate-reducing archaeon *A. fulgidus* (*20*). As observed for *Dd*27k Dsr, only four subunits were detected by SDS gel and the integral membrane subunit DsrP was not observed. A Dsr complex has also been isolated from the phototrophic *A. vinosum*. It contained mainly DsrK, DsrO, DsrE, DsrABC, and substoichiometric amounts of the cytochrome *c* subunit DsrJ, whereas the two membrane proteins DsrP and DsrM were not detected (*22*). In both the *A. fulgidus* Hme and *A. vinosum* Dsr complexes, the cytochrome *c* subunit DsrJ was only present in minor amounts or was even absent in some preparations, preventing its characterization. In contrast, the Dsr complex isolated from *Dd*27k contained stoichiometric amounts of DsrJ, enabling a more detailed investigation of this interesting protein that constitutes the first example of a novel family of multiheme cytochromes *c*. DsrJ stains poorly with Coomassie and requires a large sample load to be well-observed. However, its presence is obvious by UV−vis spectroscopy, where the hemes dominate the spectra. From analysis of the available DsrJ sequences, there are three strictly conserved residues that might act as the sixth ligand of each of the three hemes *c*: one histidine, one methionine, and one cysteine. The UV−vis and EPR spectra of the *Dd*27k Dsr hemes are compatible with each of the three hemes in DsrJ, having different coordination: one bis-His, one His/Met, and one His/Cys. This is a very unusual situation because most multiheme *c* cytochromes have bis-His coordination (*45*) and, to our knowledge, there is only one precedent for this situation, in the case of the triheme PufC cytochrome from *R. sulfidophilum* (*60*). PufC is related to the well-characterized tetraheme cytochromes of the photosynthetic reaction centers, which contain two bis-His hemes and two His/Met hemes (*64*). In PufC, one of the bis-His hemes is absent and one of the His/Met hemes has His/Cys coordination, thus having three hemes with a different coordination as DsrJ. The only other example in which a heme *c* has His/Cys coordination is in the dimeric SoxAX cytochrome that is part of the Sox enzyme system, which is involved in thiosulfate oxidation (*57*). SoxA has two hemes *c*, heme 1 with His/Cys ligation and heme 2, the active site, with His/Cys-persulfide coordination (*54*, *61*). The proposed function of the catalytic SoxA heme is to catalyze the oxidative bond formation between thiosulfate to a cysteine of the SoxY protein (*57*). The DsrJ cytochrome shows no similarity to either PufC or SoxA. However, the similar heme coordination of DsrJ and SoxA may be of relevance given the similarity between the metabolic pathways involved

(reduction versus oxidation of sulfur compounds). One important point to note is that in the Sox enzyme system the sulfur intermediates are proposed to be enzyme-bound, whereas this situation has not been considered in the sulfate reduction pathway. It is tempting to speculate whether DsrJ could be involved in sulfur chemistry. However, two points should be noted: one is that sulfate and sulfite reduction occur in the cytoplasm, whereas DsrJ is periplasmic; the other is that the His/Cys-coordinated heme of DsrJ has similar characteristics to SoxA heme 1, in terms of EPR behavior and the fact that both are redox inactive, and not to the SoxA catalytic heme 2. The actual function of the DsrJ cytochrome remains elusive. It is shown here that this cytochrome is not an electron acceptor for the H_2-oxidizing pathway in *Dd*27k with the most abundant hydrogenase and cytochrome present in this organism. For the Hme complex of *A. fulgidus*, it was proposed that the DsrJ-homologue AF503 could be reduced by menaquinol, via AF500 (DsrP) and AF499 (DsrO), and transfer electrons to an acceptor in the periplasm, possibly oxygen (*20*). However, when the *Dd*27k Dsr complex is reduced with menadiol, only 40% of the hemes are reduced, suggesting reduction of the hemes *b* but not of the DsrJ hemes *c* and thus not supporting this proposal. Nevertheless, it cannot be excluded that the DsrJ hemes may show a different behavior upon interaction with a redox partner; therefore, it remains as a question mark whether the DsrJ cytochrome is an electron entry or exit point or even a catalytic subunit for the Dsr complex.

The cytoplasmic DsrK protein is more likely to be a catalytic subunit in the Dsr complex, given its similarity to the catalytic subunit HdrD of HdrDE heterodisulfide reductases from methanogens (*36*). This suggests that DsrK may also be involved in catalyzing a thiol/disulfide type of redox chemistry. A very important point is the observation of the unusual paramagnetic species in oxidized Dsr that is also present in *A. fulgidus* Hme and which has very similar characteristics to the EPR signals observed upon binding of one of the thiol products, HS-CoM or HS-CoB, to the oxidized Hdr (*39*). In particular, the species formed by the addition of HS-CoM to the oxidized enzyme (CoM-Hdr) is believed to be an intermediate in the reaction cycle, because it has a midpoint potential (−185 mV for *M. marburgensis* Hdr) close to that of disulfide/thiol couples and it reacts with HS-CoB to form an EPR-silent form (*39*). The paramagnetic species in CoM-Hdr has been shown to be a $[4Fe-4S]^{3+}$ cluster in which one Fe site is pentacoordinated and has two thiolate ligands, one of which may be HS-CoM that binds directly to the [4Fe−4S] cluster in the active site of the enzyme (*40*−*43*). A $[4Fe-4S]^{3+}$ intermediate is also observed in ferredoxin:thioredoxin reductase, which contains a [4Fe−4S] cluster at the active site in close proximity to an active-site disulfide and performs disulfide/thiol conversion of thioredoxin by two sequential one-electron steps (*65*, *66*). One important difference observed between the paramagnetic species present both in *Dd*27k Dsr and *A. fulgidus* Hme and the $[4Fe4S]^{3+}$ signal observed in Hdr is that the former is observed in the as-isolated oxidized enzymes, whereas the latter is only observed after addition of the thiol HS-CoM. This may either be explained by the presence of a tight-binding thiol substrate in the active site of *Dd*27k DsrK and *A. fulgidus* AF502 or it may also indicate some intrinsic difference at the catalytic site relative to Hdr. The paramagnetic species could, for example, be generated by coordination of an active-site cysteine to a $[4Fe-4S]^{2+}$ cluster. The midpoint potentials for reduction of the putative $[4Fe-4S]^{3+}$ center in *Dd*27k Dsr (+130 mV) and *A. fulgidus* Hme (+90 mV) are much higher than those observed either for CoM-Hdr (−185 mV) or CoB−Hdr (−30 mV) from *M. marburgensis* and very distant from common redox potentials for disulfide/thiol couples. This indicates that the paramagnetic species observed in *Dd*27k Dsr and *A. fulgidus* Hme may not correspond to a catalytic competent state but may be a resting form generated upon oxidation.

The sequence of the Dsr complex in *Desulfovibrio* spp. predicts the presence of at least four canonical $[4Fe-4S]^{2+/1+}$ clusters, two in DsrK and two in DsrO. During the EPR redox titration of the $[4Fe-4S]^{2+/1+}$ centers, it is possible to distinguish five distinct g_{max} values using spectral subtraction, which points to the possible existence of a third $[4Fe-4S]^{2+/1+}$ cluster in DsrO. The $[4Fe-4S]^{2+/1+}$ centers are reduced in a range of potentials between 0 and −300 mV, which are not very low potentials among the family of ferredoxin-like proteins. The $[4Fe-4S]^{2+/1+}$ centers in the *A. fulgidus* Hme complex were detected only at temperatures below 10 K and redox potentials up to −100 mV (*20*), which is quite different from the behavior observed for the $[4Fe-4S]^{2+/1+}$ centers in *Dd*27K Dsr. At least one $[4Fe-4S]^{2+/1+}$ center with $g_{max} = 2.03$ is observed at 0 mV and at a temperature of 15 K, suggesting that this center has distinct properties from those present in the *A. fulgidus* Hme complex. The *A. fulgidus* Hme complex was isolated anaerobically, whereas *Dd*27K Dsr was purified aerobically. This may influence the behavior of the redox centers, but oxygen damage to Dsr is not apparent.

There is by now growing evidence to indicate that the Dsr complex is part of the same metabolic pathway that involves the sulfite reductase: all prokaryotic genomes that contain a dissimilatory sulfite reductase (DsrAB), whether they are sulfate reducers or sulfur oxidizers, contain also a DsrMKJOP membrane complex; in several genomes, the *dsrAB* and *dsrMKJOP* are part of the same gene cluster that includes other conserved *dsr* genes such as *dsrC and dsrN* (*22*); in *A. vinosum*, the DsrKJO proteins were found to associate with the DsrABC proteins (*22*); and the genes for the sulfite reductase and Dsr complex are coordinately regulated by sulfide (*21*, *22*). In this organism, the proteins encoded by the *dsr* gene cluster were shown to be essential for oxidation of intracellular stored sulfur but not for oxidation of sulfide, thiosulfate, or sulfite under photolithoautotrophic conditions (*21*, *22*). However, the precise functional role of the Dsr complex has still not been established. Sequence analysis suggests that there may be two modules in the Dsr complex, because it has two integral membrane proteins both thought to interact with the menaquinone pool (DsrM and DsrP). One module, formed by DsrM and DsrK based on its similarity to HdrED (Figure 6), could be involved in menaquinol oxidation and reduction of a cytoplasmic substrate, probably a disulfide; a second module formed by DsrP, DsrO, and DsrJ could possibly be involved in electron transfer between the menaquinone pool and a periplasmic component, but it is not clear in which direction. Although the genes coding for each of these modules are generally adjacent to each other, there is one known exception for the case of *M. thermoacetica*, where the *dsrK* gene is separated from the

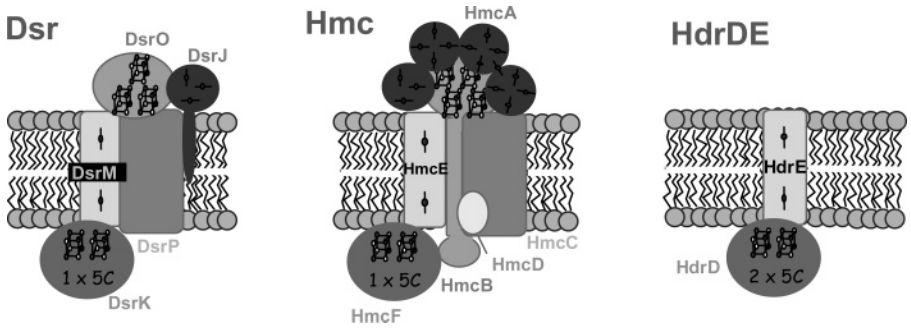

FIGURE 6: Schematic representation of *Desulfovibrio* membrane-bound complexes Dsr and Hmc and heterodisulfide reductase HdrDE, as deduced from sequence data. Related subunits are in similar shades of gray. The color code is the same as in Figure 2. 5C represents the $CX_nCCX_nCX_2C$ motif.

dsrM gene by the *dsrJOP* genes (Figure 2). This case indicates that the DsrMKJOP proteins may actually form a single functional module, which is supported by the fact that the proteins are isolated as a complex. In any case, the Dsr complex has proteins to enable interactions at the cytoplasmic, membrane, and periplasmic sites, and some of its hemes are reduced by a menaquinol analogue, suggesting that it is capable of redox reactions at the three sites.

Desulfovibrio spp. present a particularly interesting situation because they have several complexes closely related to Dsr. The genomes of *D. vulgaris* Hildenborough and *D. desulfuricans* G20 contain one copy each of the Dsr, the Hmc, and the $TpIIc_3$ complexes, which are probably related to each other (*9*). The Hmc complex composition is very similar to that of the Dsr complex in terms of the type of subunits present (Figure 6): a cytoplasmic FeS protein related to HdrD, two integral membrane proteins, a periplasmic ferredoxin-like protein, and a periplasmic cytochrome *c*. This suggests that both complexes have related functions, but the actual sequence identity between subunits is very low, indicating that the Hmc and Dsr complexes are not homologous. The multiheme cytochrome *c* subunit is the most dissimilar between the two complexes because it is a large (65 kDa), 16 heme cytochrome in Hmc and a small triheme cytochrome of 15 kDa in Dsr. The $TpIIc_3$ complex has a simpler composition in terms of redox proteins, comprising a periplasmic tetraheme cytochrome, a membrane protein of the DsrM and HmcE family, and a cytoplasmic FeS protein of the HdrD family that is related to DsrK and HmcF. In contrast to Dsr, the proteins of the Hmc and $TpIIc_3$ complexes show a high level of sequence identity between them, and despite the difference in size, the two cytochromes *c* subunits belong to the same family and have similar characteristics (*9*, *11*, *19*), whereas the DsrJ cytochrome is totally unrelated. This indicates that the Hmc and $TpIIc_3$ complexes are homologous, with the latter being a simplified version of the former. The presence of a cytoplasmic HdrD-like subunit in the three complexes, all containing a binding site for a putative catalytic [4Fe−4S] center, hints that they are implicated in similar thiol/disulfide chemistry involving the same or similar substrates.

There is no genome sequence available for *Dd*27k, and it should be noted that this organism is not closely related to *D. desulfuricans* G20, which has to be re-classified as a subspecies of *D. alaskensis*, based on 16S rRNA gene analysis (*23*). In *Dd*27k, there is no evidence for the presence of Hmc or $TpIIc_3$ complexes, but a nine-heme cytochrome (9HcA) is found that is very similar to the C-terminal domain of HmcA (*18*) and is also associated with a membrane complex (*17*). The 9Hc complex is analogous to the Hmc complex although it is missing both the heme *b* protein (HmcE) and the HdrD-like protein (HmcF). It is presently unknown whether these other proteins are either encoded somewhere else in the genome or the 9Hc complex is involved only in electron transfer between the periplasm and the membrane quinone pool.

Of all of the transmembrane complexes in *Desulfovibrio*, the Hmc is that for which more functional studies have been performed (*13*−*16*). All of these studies point to a specific role of the Hmc complex in electron transfer from periplasmic H_2 oxidation to sulfate reduction in the cytoplasm. A similar role can be presumed for the $TpIIc_3$ complex because this cytochrome is a good electron acceptor for the hydrogenase/$TpIc_3$ system (*19*). In analogy to the Hmc complex and given the difference in the cytochrome *c* subunits, we propose that the Dsr complex accepts electrons from a different periplasmic electron donor, of still unknown nature. The electron acceptor for Dsr on the cytoplasmic side may be the same as that of the Hmc and $TpIIc_3$ complexes or simply of a similar nature, given the similarity between the cytoplasmic FeS subunits. It seems likely that this electron acceptor may be a disulfide-containing species that is reduced to a thiol, which in turn could be an electron donor for the DsrAB sulfite reductase, being reoxidized to the disulfide. This thiol/disulfide could either be a small-molecular-weight compound as the HS-CoM and HS-CoB of methanogens or a thiol group of a protein. One very likely candidate for this latter case is the ~12-kDa DsrC protein that has a strictly conserved cysteine at the C terminal. DsrC contains a second cysteine at the C terminal that is conserved in all organisms that have a dissimilatory sulfite reductase but not in those organisms that only have an assimilatory sulfite reductase (*67*). In *Desulfovibrio* spp., it was shown that the purified sulfite reductase DsrAB is associated with DsrC, which was designated as the γ subunit of the sulfite reductase (*68*), and in *D. desulfuricans* Essex 6, some of the sulfite reductase was purified from the membrane fraction (*69*). However, DsrC is not co-transcribed with DsrAB (*70*) and is actually one of the most highly expressed proteins in *D. vulgaris* Hildenborough with about twice the expression level of DsrAB (*28*), pointing to an important role in cellular metabolism. Apart from DsrAB and the DsrMKJOP complex, DsrC is the only other protein that is common to all organisms containing a dissimilatory sulfite reductase, irrespective of whether they are sulfur compound reducers or oxidizers.

In conclusion, an important membrane-bound complex for sulfate respiration was isolated and characterized from the sulfate-reducing bacterium *D. desulfuricans* ATCC 27774. The present evidence indicates that this complex is involved in the respiratory electron-transfer chain and is likely to channel electrons from the periplasm and menaquinone pool to the sulfite reductase. Because sulfite reduction contributes to the generation of a proton-motive force in whole cells of *Desulfovibrio* (*71*, *72*), it is tempting to propose that electron transfer through the Dsr complex may be associated with proton translocation. Further studies are necessary to clarify the precise role of Dsr in the sulfate respiratory pathway.

ACKNOWLEDGMENT

The authors thank João Carita (ITQB) for growing the bacterial cells, Manuela Regala (ITQB) for amino acid sequencing and heme analysis, and Paula Chicau (ITQB) for amino acid analysis.

SUPPORTING INFORMATION AVAILABLE

Sequence alignments of the DsrMKJOP proteins. This material is available free of charge via the Internet at http://pubs.acs.org.

REFERENCES

1. Rabus, R., Hansen, T., and Widdel, F. (2000) Dissimilatory sulfate- and sulfur-reducing prokaryotes, in *The Prokaryotes: An Evolving Electronic Resource for the Microbiological Community* (Dworkin, M., et al., Eds.), Springer-Verlag, New York, http://link.springer-ny.com/link/service/books/10125/.
2. Jørgensen, B. B. (1982) Mineralization of organic matter in the sea-bed—The role of sulphate reduction, *Nature 390*, 364−370.
3. Hamilton, W. A. (2003) Microbially influenced corrosion as a model system for the study of metal microbe interactions: A unifying electron-transfer hypothesis, *Biofouling 19*, 65−76.
4. Dinh, H. T., Kuever, J., Mussmann, M., Hassel, A. W., Stratmann, M., and Widdel, F. (2004) Iron corrosion by novel anaerobic microorganisms, *Nature 427*, 829−832.
5. Loubinoux, J., Bronowicki, J.-P., Pereira, I. A. C., Mougenel, J.-L., and Le Faou, A. E. (2002) Sulfate-reducing bacteria in human feces and their association with inflammatory bowel diseases, *FEMS Microbiol. Lett. 40*, 107−112.
6. Lovley, D. R. (2003) Cleaning up with genomics: Applying molecular biology to bioremediation, *Nat. Rev. Microbiol. 1*.
7. Lloyd, J. R., and Renshaw, J. C. (2005) Bioremediation of radioactive waste: Radionuclide−microbe interactions in laboratory and field-scale studies, *Curr. Opin. Biotechnol. 16*, 254−260.
8. Gibson, J., and C, S. H. (2002) Metabolic diversity in aromatic compound utilization by anaerobic microbes, *Annu. Rev. Microbiol. 56*, 345−369.
9. Matias, P. M., Pereira, I. A. C., Soares, C. M., and Carrondo, M. A. (2005) Sulphate respiration from hydrogen in *Desulfovibrio* bacteria: A structural biology overview, *Prog. Biophys. Mol. Biol. 89*, 292−329.
10. Rossi, M., Pollock, W. B. R., Reij, M. W., Keon, R. G., Fu, R., and Voordouw, G. (1993) The hmc operon of *Desulfovibrio vulgaris* subsp. *vulgaris* Hildenborough encodes a potential transmembrane redox protein complex, *J. Bacteriol. 175*, 4699−4711.
11. Matias, P. M., Coelho, A. V., Valente, F. M. A., D., P., LeGall, J., Xavier, A. V., Pereira, I. A. C., and Carrondo, M. A. (2002) Sulfate respiration in *Desulfovibrio vulgaris* Hildenborough: Structure of the 16-heme cytochrome *c* HmcA at 2.5 Å resolution and a view of its role in transmembrane electron transfer, *J. Biol. Chem. 277*, 47907−47916.
12. Czjzek, M., ElAntak, L., Zamboni, V., Morelli, X., Dolla, A., Guerlesquin, F., and Bruschi, M. (2002) The crystal structure of the hexadeca-heme cytochrome Hmc and a structural model of its complex with cytochrome c_3, *Structure 10*, 1677−1686.
13. Keon, R. G., Fu, R., and Voordouw, G. (1997) Deletion of two downstream genes alters expression of the hmc operon of *Desulfovibrio vulgaris* subsp. *vulgaris* Hildenborough, *Arch. Microbiol. 167*, 376−383.
14. Dolla, A., Pohorelic, B. K., Voordouw, J. K., and Voordouw, G. (2000) Deletion of the hmc operon of *Desulfovibrio vulgaris* subsp. *vulgaris* Hildenborough hampers hydrogen metabolism and low-redox-potential niche establishment, *Arch. Microbiol. 174*, 143−151.
15. Voordouw, G. (2002) Carbon monoxide cycling by *Desulfovibrio vulgaris* Hildenborough, *J. Bacteriol. 184*, 5903−5911.
16. Pereira, I. A. C., Romão, C. V., Xavier, A. V., LeGall, J., and Teixeira, M. (1998) Electron transfer between hydrogenases and mono and multiheme cytochromes in *Desulfovibrio* spp., *J. Biol. Inorg. Chem. 3*, 494−498.
17. Saraiva, L. M., da Costa, P. N., Conte, C., Xavier, A. V., and LeGall, J. (2001) In the facultative sulphate/nitrate reducer *Desulfovibrio desulfuricans* ATCC 27774, the nine-haem cytochrome *c* is part of a membrane-bound redox complex mainly expressed in sulphate-grown cells, *Biochim. Biophys. Acta 1520*, 63−70.
18. Matias, P. M., Coelho, R., Pereira, I. A., Coelho, A. V., Thompson, A. W., Sieker, L. C., Gall, J. L., and Carrondo, M. A. (1999) The primary and three-dimensional structures of a nine-haem cytochrome *c* from *Desulfovibrio desulfuricans* ATCC 27774 reveal a new member of the Hmc family, *Structure 7*, 119−130.
19. Valente, F. M. A., Saraiva, L. M., LeGall, J., Xavier, A. V., Teixeira, M., and Pereira, I. A. C. (2001) A membrane-bound cytochrome c_3: A type II cytochrome c_3 from *Desulfovibrio vulgaris* Hildenborough, *ChemBioChem 2*, 895−905.
20. Mander, G. J., Duin, E. C., Linder, D., Stetter, K. O., and Hedderich, R. (2002) Purification and characterization of a membrane-bound enzyme complex from the sulfate-reducing archaeon *Archaeoglobus fulgidus* related to heterodisulfide reductase from methanogenic archaea, *Eur. J. Biochem. 269*, 1895−1904.
21. Pott, A. S., and Dahl, C. (1998) Sirohaem sulfite reductase and other proteins encoded by genes at the dsr locus of *Chromatium vinosum* are involved in the oxidation of intracellular sulfur, *Microbiology 144*, 1881−1894.
22. Dahl, C., Engels, S., Pott-Sperling, A. S., Schulte, A., Sander, J., Lubbe, Y., Deuster, O., and Brune, D. C. (2005) Novel genes of the dsr gene cluster and evidence for close interaction of Dsr proteins during sulfur oxidation in the phototrophic sulfur bacterium *Allochromatium vinosum*, *J. Bacteriol. 187*, 1392−1404.
23. Pires, R. H., Lourenco, A. I., Morais, F., Teixeira, M., Xavier, A. V., Saraiva, L. M., and Pereira, I. A. (2003) A novel membrane-bound respiratory complex from *Desulfovibrio desulfuricans* ATCC 27774, *Biochim. Biophys. Acta 1605*, 67−82.
24. Haveman, S. A., Greene, E. A., Stilwell, C. P., Voordouw, J. K., and Voordouw, G. (2004) Physiological and gene expression analysis of inhibition of *Desulfovibrio vulgaris* Hildenborough by nitrite, *J. Bacteriol. 186*, 7944−7950.
25. Klenk, H. P., Clayton, R. A., Tomb, J. F., White, O., Nelson, K. E., Ketchum, K. A., Dodson, R. J., Gwinn, M., Hickey, E. K., Peterson, J. D., Richardson, D. L., Kerlavage, A. R., Graham, D. E., Kyrpides, N. C., Fleischmann, R. D., Quackenbush, J., Lee, N. H., Sutton, G. G., Gill, S., Kirkness, E. F., Dougherty, B. A., McKenney, K., Adams, M. D., Loftus, B., Venter, J. C., et al. (1997) The complete genome sequence of the hyperthermophilic, sulphate-reducing archaeon *Archaeoglobus fulgidus*, *Nature 390*, 364−370.
26. Heidelberg, J. F., Seshadri, R., Haveman, S. A., Hemme, C. L., Paulsen, I. T., Kolonay, J. F., Eisen, J. A., Ward, N., Methe, B., Brinkac, L. M., Daugherty, S. C., Deboy, R. T., Dodson, R. J., Durkin, A. S., Madupu, R., Nelson, W. C., Sullivan, S. A., Fouts, D., Haft, D. H., Selengut, J., Peterson, J. D., Davidsen, T. M., Zafar, N., Zhou, L. W., Radune, D., Dimitrov, G., Hance, M., Tran, K., Khouri, H., Gill, J., Utterback, T. R., Feldblyum, T. V., Wall, J. D., Voordouw, G., and Fraser, C. M. (2004) The genome sequence of the anaerobic, sulfate-reducing bacterium *Desulfovibrio vulgaris* Hildenborough, *Nat. Biotechnol. 22*, 554−559.
27. Rabus, R., Ruepp, A., Frickey, T., Rattei, T., Fartmann, B., Stark, M., Bauer, M., Zibat, A., Lombardot, T., Becker, I., Amann, J., Gellner, K., Teeling, H., Leuschner, W. D., Glockner, F. O., Lupas, A. N., Amann, R., and Klenk, H. P. (2004) The genome of

Desulfotalea psychrophila, a sulfate-reducing bacterium from permanently cold Arctic sediments, *Environ. Microbiol. 6*, 887−902.
28. Haveman, S. A., Brunelle, V., Voordouw, J. K., Voordouw, G., Heidelberg, J. F., and Rabus, R. (2003) Gene expression analysis of energy metabolism mutants of *Desulfovibrio vulgaris* Hildenborough indicates an important role for alcohol dehydrogenase, *J. Bacteriol. 185*, 4345−4353.
29. Berry, E. A., and Trumpower, B. L. (1987) Simultaneous determination of hemes a, b, and c from pyridine hemochrome spectra, *Anal. Biochem. 161*, 1−15.
30. Lubben, M., and Morand, K. (1994) Novel prenylated hemes as cofactors of cytochrome oxidases. Archaea have modified hemes A and O, *J. Biol. Chem. 269*, 21473−21479.
31. Fisher, D. S., and Price, D. C. (1964) A simple serum iron method using the new sensitive chromogen trypiridyl-*s*-triazine, *Clin. Chem. 10*, 21−31.
32. Snyder, C. H., and Trumpower, B. L. (1999) Ubiquinone at center N is responsible for triphasic reduction of cytochrome *b* in the cytochrome bc_1 complex, *J. Biol. Chem. 274*, 31209−31216.
33. Price, M. N., Huang, K. H., Alm, E. J., and Arkin, A. P. (2005) A novel method for accurate operon predictions in all sequenced prokaryotes, *Nucleic Acids Res. 33*, 880−892.
34. Berks, B. C., Page, M. D., Richardson, D. J., Reilly, A., Cavill, A., Outen, F., and Ferguson, S. J. (1995) Sequence analysis of subunits of the membrane-bound nitrate reductase from a denitrifying bacterium: The integral membrane subunit provides a prototype for the dihaem electron-carrying arm of a redox loop, *Mol. Microbiol. 15*, 319−331.
35. Bertero, M. G., Rothery, R. A., Palak, M., Hou, C., Lim, D., Blasco, F., Weiner, J. H., and Strynadka, N. C. (2003) Insights into the respiratory electron-transfer pathway from the structure of nitrate reductase A, *Nat. Struct. Biol. 10*, 681−687.
36. Kunkel, A., Vaupel, M., Heim, S., Thauer, R. K., and Hedderich, R. (1997) Heterodisulfide reductase from methanol-grown cells of *Methanosarcina barkeri* is not a flavoenzyme, *Eur. J. Biochem. 244*, 226−234.
37. Hedderich, R., Klimmek, O., Kroger, A., Dirmeier, R., Keller, M., and Stetter, K. O. (1999) Anaerobic respiration with elemental sulfur and with disulfides, *FEMS Microbiol. Rev. 22*, 353−381.
38. Lemos, R. S., Fernandes, A. S., Pereira, M. M., Gomes, C. M., and Teixeira, M. (2002) Quinol:fumarate oxidoreductases and succinate:quinone oxidoreductases: Phylogenetic relationships, metal centres and membrane attachment, *Biochim. Biophys. Acta 1553*, 158−170.
39. Madadi-Kahkesh, S., Duin, E. C., Heim, S., Albracht, S. P., Johnson, M. K., and Hedderich, R. (2001) A paramagnetic species with unique EPR characteristics in the active site of heterodisulfide reductase from methanogenic archaea, *Eur. J. Biochem. 268*, 2566−2577.
40. Duin, E. C., Madadi-Kahkesh, S., Hedderich, R., Clay, M. D., and Johnson, M. K. (2002) Heterodisulfide reductase from Methanothermobacter marburgensis contains an active-site [4Fe−4S] cluster that is directly involved in mediating heterodisulfide reduction, *FEBS Lett. 512*, 263−268.
41. Duin, E. C., Bauer, C., Jaun, B., and Hedderich, R. (2003) Coenzyme M binds to a [4Fe−4S] cluster in the active site of heterodisulfide reductase as deduced from EPR studies with the [33S]coenzyme M-treated enzyme, *FEBS Lett. 538*, 81−84.
42. Bennati, M., Weiden, N., Dinse, K. P., and Hedderich, R. (2004) (57)Fe ENDOR spectroscopy on the iron−sulfur cluster involved in substrate reduction of heterodisulfide reductase, *J. Am. Chem. Soc. 126*, 8378−8379.
43. Shokes, J. E., Duin, E. C., Bauer, C., Jaun, B., Hedderich, R., Koch, J., and Scott, R. A. (2005) Direct interaction of coenzyme M with the active-site Fe−S cluster of heterodisulfide reductase, *FEBS Lett. 579*, 1741−1744.
44. Mori, H., and Ito, K. (2001) The Sec protein-translocation pathway, *Trends Microbiol. 9*, 494−500.
45. Pereira, I. A. C., and Xavier, A. V. (2005) Multi-heme c cytochromes and enzymes, in *Encyclopedia of Inorganic Chemistry* (King, R. B., Ed.) John Wiley and Sons, New York.
46. Berks, B. C., Palmer, T., and Sargent, F. (2005) Protein targeting by the bacterial twin-arginine translocation (Tat) pathway, *Curr. Opin. Microbiol. 8*, 174−181.
47. Keon, R. G., and Voordouw, G. (1996) Identification of the HmcF and topology of the HmcB subunit of the Hmc complex of *Desulfovibrio vulgaris*, *Anaerobe 2*, 231−238.
48. Menon, N. K., Chatelus, C. Y., Dervartanian, M., Wendt, J. C., Shanmugam, K. T., Peck, H. D., Jr., and Przybyla, A. E. (1994) Cloning, sequencing, and mutational analysis of the hyb operon encoding *Escherichia coli* hydrogenase 2, *J. Bacteriol. 176*, 4416−4423.
49. Fisher, N., and Rich, P. R. (2000) A motif for quinone binding sites in respiratory and photosynthetic systems, *J. Mol. Biol. 296*, 1153−1162.
50. Mander, G. J., Pierik, A. J., Huber, H., and Hedderich, R. (2004) Two distinct heterodisulfide reductase-like enzymes in the sulfate-reducing archaeon *Archaeoglobus profundus*, *Eur. J. Biochem. 271*, 1106−1116.
51. Dhawan, I. K., Shelver, D., Thorsteinsson, M. V., Roberts, G. P., and Johnson, M. K. (1999) Probing the heme axial ligation in the CO-sensing CooA protein with magnetic circular dichroism spectroscopy, *Biochemistry 38*, 12805−12813.
52. Lanzilotta, W. N., Schuller, D. J., Thorsteinsson, M. V., Kerby, R. L., Roberts, G. P., and Poulos, T. L. (2000) Structure of the CO sensing transcription activator CooA, *Nat. Struct. Biol. 7*, 876−880.
53. Ojha, S., Hwang, J., Kabil, O., Penner-Hahn, J. E., and Banerjee, R. (2000) Characterization of the heme in human cystathionine β-synthase by X-ray absorption and electron paramagnetic resonance spectroscopies, *Biochemistry 39*, 10542−10547.
54. Cheesman, M. R., Little, P. J., and Berks, B. C. (2001) Novel heme ligation in a c-type cytochrome involved in thiosulfate oxidation: EPR and MCD of SoxAX from *Rhodovulum sulfidophilum*, *Biochemistry 40*, 10562−10569.
55. Dawson, J. H., Andersson, L. A., and Sono, M. (1982) Spectroscopic investigations of ferric cytochrome P-450_{cam} ligand complexes. Identification of the ligand trans to cysteinate in the native enzyme, *J. Biol. Chem. 257*, 3606−3617.
56. Tsai, A. L., Berka, V., Chen, P. F., and Palmer, G. (1996) Characterization of endothelial nitric-oxide synthase and its reaction with ligand by electron paramagnetic resonance spectroscopy, *J. Biol. Chem. 271*, 32563−32571.
57. Friedrich, C. G., Bardischewsky, F., Rother, D., Quentmeier, A., and Fischer, J. (2005) Prokaryotic sulfur oxidation, *Curr. Opin. Microbiol. 8*, 253−259.
58. Kappler, U., Aguey-Zinsou, K. F., Hanson, G. R., Bernhardt, P. V., and McEwan, A. G. (2004) Cytochrome *c*551 from *Starkeya novella*: Characterization, spectroscopic properties, and phylogeny of a diheme protein of the SoxAX family, *J. Biol. Chem. 279*, 6252−6260.
59. Kelly, D. P., Shergill, J. K., Lu, W. P., and Wood, A. P. (1997) Oxidative metabolism of inorganic sulfur compounds by bacteria, *Antonie Van Leeuwenhoek 71*, 95−107.
60. Alric, J., Tsukatani, Y., Yoshida, M., Matsuura, K., Shimada, K., Hienerwadel, R., Schoepp-Cothenet, B., Nitschke, W., Nagashima, K. V., and Vermeglio, A. (2004) Structural and functional characterization of the unusual triheme cytochrome bound to the reaction center of *Rhodovulum sulfidophilum*, *J. Biol. Chem. 279*, 26090−26097.
61. Bamford, V. A., Bruno, S., Rasmussen, T., Appia-Ayme, C., Cheesman, M. R., Berks, B. C., and Hemmings, A. M. (2002) Structural basis for the oxidation of thiosulfate by a sulfur cycle enzyme, *EMBO J. 21*, 5599−5610.
62. Tsai, R., Yu, C. A., Gunsalus, I. C., Peisach, J., Blumberg, W., Orme-Johnson, W. H., and Beinert, H. (1970) Spin-state changes in cytochrome P-450_{cam} on binding of specific substrates, *Proc. Natl. Acad. Sci. U.S.A. 66*, 1157−1163.
63. Lipscomb, J. D. (1980) Electron paramagnetic resonance detectable states of cytochrome P-450_{cam}, *Biochemistry 19*, 3590−3599.
64. Lancaster, C. R. D., and Michel, H. (2001) Photosynthetic reaction centers of purple bacteria, in *Handbook of Metalloproteins* (Messerschmidt, A., Huber, R., Poulos, T., and Wieghardt, K., Eds.) pp 119−135, Wiley, New York.
65. Dai, S., Schwendtmayer, C., Schurmann, P., Ramaswamy, S., and Eklund, H. (2000) Redox signaling in chloroplasts: Cleavage of disulfides by an iron−sulfur cluster, *Science 287*, 655−658.
66. Walters, E. M., Garcia-Serres, R., Jameson, G. N., Glauser, D. A., Bourquin, F., Manieri, W., Schurmann, P., Johnson, M. K., and Huynh, B. H. (2005) Spectroscopic characterization of site-specific [Fe(4)S(4)] cluster chemistry in ferredoxin:thioredoxin reductase: Implications for the catalytic mechanism, *J. Am. Chem. Soc. 127*, 9612−9624.
67. Cort, J. R., Mariappan, S. V., Kim, C. Y., Park, M. S., Peat, T. S., Waldo, G. S., Terwilliger, T. C., and Kennedy, M. A. (2001) Solution structure of *Pyrobaculum aerophilum* DsrC, an archaeal

homologue of the γ subunit of dissimilatory sulfite reductase, *Eur. J. Biochem. 268*, 5842−5850.
68. Pierik, A. J., Duyvis, M. G., van Helvoort, J. M., Wolbert, R. B., and Hagen, W. R. (1992) The third subunit of desulfoviridin-type dissimilatory sulfite reductases, *Eur. J. Biochem. 205*, 111−115.
69. Steuber, J., Arendsen, A. F., Hagen, W. R., and Kroneck, P. M. (1995) Molecular properties of the dissimilatory sulfite reductase from *Desulfovibrio desulfuricans* (Essex) and comparison with the enzyme from *Desulfovibrio vulgaris* (Hildenborough), *Eur. J. Biochem. 233*, 873−879.
70. Karkhoff-Schweizer, R. R., Bruschi, M., and Voordouw, G. (1993) Expression of the γ-subunit gene of desulfoviridin-type dissimilatory sulfite reductase and of the α- and β-subunit genes is not coordinately regulated, *Eur. J. Biochem. 211*, 501−507.
71. Fitz, R. M., and Cypionka, H. (1989) A study on electron transport-driven proton translocation in *Desulfovibrio desulfuricans*, *Arch. Microbiol. 152*, 369−376.
72. Fitz, R. M., and Cypionka, H. (1991) Generation of a proton gradient in *Desulfovibrio vulgaris*, *Arch. Microbiol. 155*, 444−448.

BI0515265